Industrial and Systems Engineering

New Estimators of the Hurst Index for Fractional Brownian Motion

Robert H. Storer
Lehigh University

Daniel J. Scansaroli
Lehigh University

Vladimir Dobrić
Lehigh University

Report: 11T-004

New Estimators of the Hurst Index for Fractional Brownian Motion

Vladimir Dobrić*
Department of Mathematics

Daniel J. Scansaroli†
Department of Industrial Engineering

Robert H. Storer †
Department of Industrial Engineering

Lehigh University ‡

Abstract

In this paper we introduce three new consistent estimators of the Hurst index for fractional Brownian motion (fBm) using ergodic theory for stochastic processes. We derive closed form solutions that are computationally faster than all methods know to the authors. These new estimators allow for the estimation of the parameters of a fractional Wiener process with unknown and constant drift, scale and Hurst index. Robustness of these estimators is also explored. Using Monte Carlo simulation, we perform an empirical study of the ergodic estimators, Peng's Variance of Residuals Method [10] and Whittle's approximate MLE [12, 1]. Our study demonstrates that the ergodic estimators outperform Peng's method and are very competitive to Whittle's estimates in terms of RMSE. We demonstrate the versatility of the ergodic estimation techniques to accommodate different data structures; i.e. standard fractional Brownian motion or a fractional Wiener process with unknown drift and scale.

1 Introduction

Modeling with fractional Brownian motion (fBm) requires reliable estimation of the Hurst index. Applications in finance, biology or network flows often require both speed and accuracy in parameter estimation for small samples in order to facilitate dynamic decision making and risk management. Fractional Brownian motion's weak derivative (or increments) with respect to time is known as fractional Gaussian noise (fGn). The self-similar and stationary properties of fractional Gaussian noise make the process a perfect candidate for the use of ergodic theory to estimate parameters influencing the behavior of these models.

*Department of Mathematics, 14 West Packer Ave., Lehigh University, Bethlehem, PA 18015
†Department of Industrial and Systems Engineering, 200 West Packer Ave., Lehigh University, Bethlehem, PA 18015
‡The authors are thankful to Dr. Wei-Min Huang of the Mathematics Department for his helpful suggestions.

Taqqu et al. [11] gives a summary of several previously proposed estimators of the Hurst index and estimates their relative accuracy for large sample sizes via Monte-Carlo simulations. These estimators typically are derived using the properties of the behavior of the spectral density of fBm, estimated through a periodogram. Other simpler methods take advantage of the asymptotic behavior of the process in the time domain. The ergodic estimators of the Hurst index for fBm introduced in this paper are shown to be competitive to the top performers in Taqqu's paper in terms of both RMSE and computational time.

2 New Estimators for the Hurst Index

We start by estimating the Hurst index for fractional Brownian motion using an L^2 norm calculation. We expand on this method by considering a more realistic model where the fractional Brownian motion process (fBm) is subject to unknown scale and drift. Throughout this section we will use the notation $\{W_i^H\}_{i=0}^N$ to represent a discrete realization of $N+1$ observations of a fractional Brownian motion process with Hurst index H.

Definition 1. Let $0 < H < 1$. A standard fractional Brownian motion (fBm) $W^H = \{W_t^H\}_{t\in\mathbb{R}}$is a centered Gaussian process with the following properties:

1. $W_0^H = 0$ almost surely.
2. $W_t^H - W_s^H$ is distributed as $N\left(0, |t-s|^{2H}\right)$.
3. $t \to W_t^H$ is continuous almost surely.

By definition, $\{W_{i+1}^H - W_i^H\} \stackrel{d}{=} N_i\left(0, \Delta t^{2H}\right)$, where Δt is a constant unit of time between W_{i+1}^H and W_i^H.

Let $X =< W_1^H - W_o^H, W_2^H - W_1^H, W_3^H - W_2^H, \ldots, W_N^H - W_{N-1}^H, \cdots >$ and let f be any Borel function with $\mathbb{E}\left[f\left(W_1^H\right)\right] < \infty$. Then,

$$\frac{1}{N}\sum_{i=0}^{N} f\left(W_{i+1}^H - W_i^H\right) \to \mathbb{E}\left[f\left(W_1^H - W_o^H\right)\right]$$

converges almost surely (a.s.) since the fGn process, X, is ergodic and a stationary sequence ([14], 131-132).

2.1 Ergodic Theory and Hurst Index Estimation

Let us set $f(x) = |x|^k$, $k \in \mathbb{R}^+$. By ergodic theory and properties of fGn, we have

$$\frac{1}{N}\sum_{i=0}^{N-1} \left|W_{i+1}^H - W_i^H\right|^k \quad \to \quad \mathbb{E}[W_1^H]^k,\ a.s. \tag{1}$$

and since the increments of fGn are Gaussian

$$\mathbb{E}[W_1^H]^k = \Delta t^{2H}\left[\frac{2^{k/2}\Gamma\left(\frac{k+1}{2}\right)}{\Gamma\left(\frac{1}{2}\right)}\right].$$

Note that the use of the k^{th} moment for estimating the Hurst index is not the result of the maximum likelihood estimation (MLE) formulations. Ergodic theory gives us no information about the bias of the estimate. If we are given any realization of a fractional Brownian motion time series $\{W_i\}_{i=0}^N$, we can apply ergodic theory to estimate the Hurst index by using the second moment of a normal distribution. Solving for H, we obtain:

$$\hat{H} = \frac{\log\left\{\frac{1}{N}\sum_{i=0}^{N-1}\left(W_{i+1}^H - W_i^H\right)^2\right\}}{2\log(\Delta t)}. \tag{2}$$

Peltier [9] shows (through the use of box dimension analysis) that absolute moment estimators of the Hurst index all perform well. However the second moment yields the most accurate estimators in terms of RMSE. In §4.1, we give numerical results in which we compare the "Second Moment" method to Whittle's approximate MLE and Peng's Variance of Residuals method. We empirically demonstrate that the ergodic estimator using the second moment is superior to Whittle's method in terms of RMSE and far better in terms of computational time, however this method can only be used when the scale and location of the fBm process are known.

2.2 Parameter Estimation in a Fractional Wiener Process

Real world data does not follow a standard fBm model. In this section we derive methods to estimate the Hurst index when the fBm is not standard, but is influenced by unknown scale and drift. Let $\{X_i\}_{i=1}^N$ be a fractional Wiener process that is $X_i \equiv \mu\Delta t + \sigma\left(W_{i+1}^H - W_i^H\right)$. Since $X_i \overset{d}{=} N_i\left(\mu\Delta t, \sigma^2(\Delta t)^{2H}\right)$, an estimate of the drift μ can be found using ergodic theory as

$$\hat{\mu} = \frac{1}{N\Delta t}\sum_{i=1}^{N} X_i \rightarrow \frac{\mathbb{E}\left[N\left(\mu\Delta t, \sigma^2(\Delta t)^{2H}\right)\right]}{\Delta t}. \tag{3}$$

We can use the location estimate to obtain a scaled fractional Gaussian noise process, $X_i - \hat{\mu}\Delta t = \sigma\left(W_{i+1}^H - W_i^H\right)$. In the next sub-sections, we introduce new ergodic estimators of the the Hurst index when fGn is influenced by an unknown scale σ.

2.2.1 Ratio of Second Moments Method

If fBm is only affected by a scale factor, the second moment converges by ergodic theory to $\sigma^2(\Delta t)^{2H}$:

$$SS_1 \equiv \frac{1}{N} \sum_{i=0}^{N-1} \sigma^2 \left(W_{i+1}^H - W_i^H \right)^2 \to \sigma^2 (\Delta t)^{2H}. \tag{4}$$

If we form stationary processes on disjoint sets of length $2\Delta t$, then we can once again use the ergodic second moment to define two estimates; one formed from the even increments and the other from the odd increments:

$$SS_{even} \equiv \frac{1}{\lfloor N/2 \rfloor} \sum_{i=0}^{\lfloor N/2 \rfloor - 1} \sigma^2 \left(W_{2i+2}^H - W_{2i}^H \right)^2 \to \sigma^2 (2\Delta t)^{2H}, \tag{5}$$

$$SS_{odd} \equiv \frac{1}{\lfloor N/2 \rfloor} \sum_{i=0}^{\lfloor N/2 \rfloor - 1} \sigma^2 \left(W_{2i+3}^H - W_{2i+1}^H \right)^2 \to \sigma^2 (2\Delta t)^{2H}. \tag{6}$$

To reduce the error of the $\sigma^2 (2\Delta t)^{2H}$ estimate, and utilize all information available in the time series, the even and odd estimates are averaged. Both the even and the odd estimators use the data set and thus these two estimators have the same variance. Therefore, the average of theses two estimators reduces the variance and bias:

$$SS_2 \equiv \frac{SS_{even} + SS_{odd}}{2} \to \sigma^2 (2\Delta t)^{2H}. \tag{7}$$

Notice that for a fractional Wiener process, the second moment estimator converges to

$$\begin{aligned} \mathbb{E}\left[X_i^2\right] &= \mu^2 (\Delta t)^2 + 2\mu \Delta t \sigma \mathbb{E}\left[W_{i+1}^H - W_i^H\right] \\ &\quad + \sigma^2 \mathbb{E}\left[\left(W_{i+1}^H - W_i^H\right)^2\right] \qquad (8) \\ &= \mu^2 (\Delta t)^2 + \sigma^2 (\Delta t)^{2H}. \qquad (9) \end{aligned}$$

Additionally, when Δt is small $\mu^2 (\Delta t)^2 \ll \sigma^2 (\Delta t)^{2H}$, if $\mu \approx 0$. Therefore, when estimating $\mathbb{E}\left[X_i^2\right]$ with small Δt, an estimate of μ may not be needed. In this situation the term $\mu^2 (\Delta t)^2$ would contribute to the error ϵ of the estimate and we can proceed using equation 7 directly, where

$$\mathbb{E}\left[X_i^2\right] = \sigma^2 (\Delta t)^{2H} + \epsilon. \tag{10}$$

Note that even if $\Delta t \ll 1$, as H increases the magnitude of $\sigma^2 (\Delta t)^{2H}$ relative to the error ϵ becomes closer. Taking a ratio of the two moments SS_1 (equation 4) and SS_2 (equation 7) the scaling and time factors cancel and we obtain:

$$\frac{SS_2}{SS_1} = 2^{2H} \implies \hat{H} = \frac{\log\left(\frac{SS_2}{SS_1}\right)}{2\log(2)}. \tag{11}$$

This estimator of H is based on the ratio of two second moments, therefore we refer to this method as the "Ratio method". The Ratio method's estimate of H can be applied in equation 4 to estimate the scale influence the fractional Wiener process, $\hat{\sigma}$:

$$\hat{\sigma} = \sqrt{\frac{SS_1}{(\Delta t)^{2\hat{H}}}} \tag{12}$$

In §4.2 we show the results of Monte Carlo simulations of a fractional Wiener Process to evaluate the performance of the Ratio method estimator. It should be noted that application of this method on real data requires filtering of any identifiable outliers or jumps, since a large jump will skew SS_1 and SS_2 and therefore bias the estimation of the Hurst index. The Ratio method is sensitive to these types of anomalies in data, as discussed in §3. The error in the Ratio method's estimates of H and σ are highly correlated, which is evident from the method used. The same kind of estimators can be derived using different combinations of the higher moments in equation 1 to estimate the Hurst index for a fractional Wiener process. These estimators can be shown to be equivalent to or worse than the Ratio method.

2.2.2 Quadrant Method

In this section we introduce an estimator which is more robust to outliers and jumps and which (unlike the Ratio method) does not depend on σ. Let us consider a fractional Wiener process with no drift (μ=0),

$$X_i = \sigma\left(W_{i+1}^H - W_i^H\right). \tag{13}$$

Note that the process $\{X_i\}_{i=1}^N$ is mean zero. If the data set being analyzed has drift, an estimate of drift will need to be made using equation 3.

Figure 1:

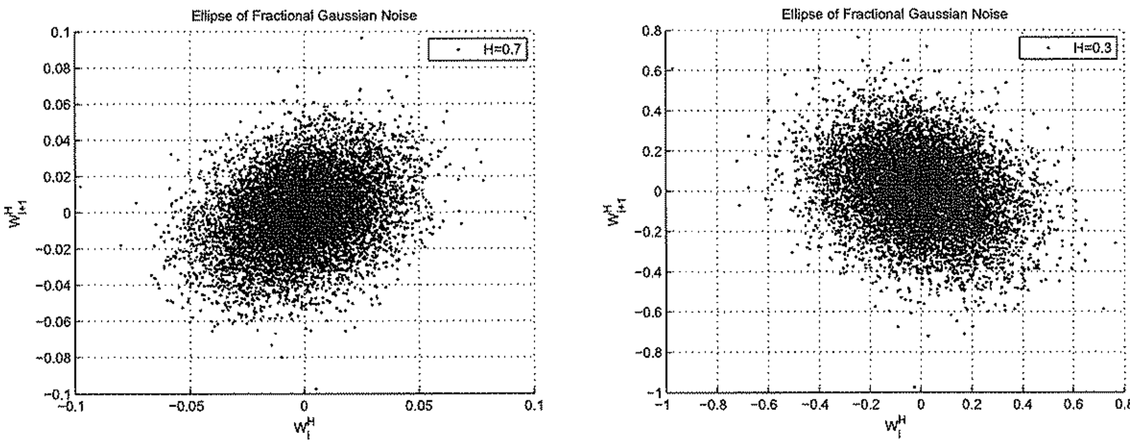

Two consecutive observations of fGn are normally distributed with Pearson's correlation coefficient $\rho = 2^{2H-1} - 1$. A 2-D plot of consecutive random observations of fGn is shaped like an ellipse (or a circle when $H = 1/2$) at a constant probability level. The Hurst index of the process (and the probability level) directly dictates the length of the axes of the bi-variate normal distribution (see Figure 1). The shape of the ellipse (or in this case the relative density in any particular quadrant of the 2-D plot) can be used to estimate the Hurst index. The major axis of the ellipse is always at $\pm\frac{\pi}{4}$ with respect to the positive or negative auto-correlation of the process, respectively.

Let us define a new process $\{Z_i\}_{i=1}^{N}$ by

$$Z_i \equiv sgn\,(X_i)\, sgn\,(X_{i+1})\,,$$

where $sgn\,(x) = 1$ if $x > 0$, and $sgn\,(x) = -1$ if $x < 0$, and $sgn\,(x) = 0$ if $x = 0$.

The signum function only sees sign and not magnitude of X_i, therefore σ does not affect the estimation of H. To estimate the Hurst index we need to compute the expected value of the process Z_i. This can be accomplished using ergodic theory. Notice,

$$\mathbb{E}\,[Z_i] = \mathbb{E}\left[\frac{X_i}{\sqrt{X_i^2}}\frac{X_{i+1}}{\sqrt{X_{i+1}^2}}\right]. \tag{14}$$

Since $\{X_i\}$ is a scaled fractional Gaussian noise, it is normally distributed with mean zero and variance $\sigma^2\Delta t^{2H}$, with correlation between X_i and X_{i+1} given by $\rho = 2^{2H-1} - 1$, therefore, the expected value converges to

$$\mathbb{E}\left[Z_i\right] = \frac{1}{2\pi D^{1/2}} \int_{-\infty}^{\infty} \int_{-\infty}^{\infty} \frac{xy}{|x||y|} e^{-\frac{1}{2D}\left(x^2 - 2xy\rho + y^2\right)} dx\, dy, \tag{15}$$

where $D = (1 - \rho^2)$.

Analytically, the expected value (equation 15) is the same as the probability that two consecutive observations of fractional Gaussian noise (X_i and X_{i+1}) are in the same diagonal quadrants of a two dimensional graph of X_i verses X_{i+1}. Each Z results in four outcomes. We refer to this technique as the "Quadrant method." Equation 15 becomes,

$$\begin{aligned} \mathbb{E}[Z_i] &= P\left(X \geq 0, Y \geq 0\right) + P\left(X < 0, Y < 0\right) \\ &\quad - P\left(X \geq 0, Y < 0\right) - P\left(X < 0, Y \geq 0\right). \end{aligned} \tag{16}$$

Utilizing the symmetry of the two dimensional Gaussian distribution,

$$\mathbb{E}\left[Z_i\right] = 2 * P\left(X \geq 0, Y \geq 0\right) - 2 * P\left(X \geq 0, Y < 0\right). \tag{17}$$

Let $u = \frac{x}{\sqrt{D}}$ and$v = \frac{y}{\sqrt{D}}$ then,

$$\mathbb{E}\left[Z_i\right] = \frac{\sqrt{D}}{2\pi} \int_{-\infty}^{\infty} \int_{-\infty}^{\infty} \frac{uv}{|u||v|} e^{-\frac{1}{2}\left(u^2 - 2uv\rho + v^2\right)} du\, dv, \tag{18}$$

and equation 17 becomes,

$$\mathbb{E}\left[Z_i\right] = 2\sqrt{D}\left[P\left(U \geq 0, V \geq 0\right) - P\left(U \geq 0, V < 0\right)\right]. \tag{19}$$

The first term in equation 17 yields

$$P\left(U \geq 0, V \geq 0\right) = \frac{1}{2\pi} \int_0^{\infty} \int_0^{\infty} e^{-\frac{1}{2}\left(u^2 - 2uv\rho + v^2\right)} du\, dv \tag{20}$$

$$= \frac{1}{\sqrt{2\pi}} \int_0^{\infty} \frac{1}{\sqrt{2\pi}} \int_{-v\rho}^{\infty} e^{-\frac{1}{2}(u - v\rho)^2} du\, e^{-\frac{1}{2}\left(v^2 - \rho^2 v^2\right)} dv. \tag{21}$$

Let $x = u - v\rho$, then

$$P(U \geq 0, V \geq 0) = \frac{1}{\sqrt{2\pi}} \int_0^\infty \frac{1}{\sqrt{2\pi}} \int_0^\infty e^{-\frac{x^2}{2}} dx \, e^{-\frac{1}{2}\left(v^2 - \rho^2 v^2\right)} dv, \tag{22}$$

$$= \frac{1}{\sqrt{2\pi}} \int_0^\infty \Phi(vp) \, e^{-\frac{1}{2}\left(v^2 - \rho^2 v^2\right)} dv. \tag{23}$$

where $\Phi(vp) = P(N(0,1) < vp)$. Substituting $y = v\rho$,

$$P(U \geq 0, V \geq 0) = \frac{1}{\sqrt{2\pi}\rho} \int_0^\infty \Phi(y) \; e^{-\frac{y^2}{2}\left(\frac{1-\rho^2}{\rho^2}\right)} dy. \tag{24}$$

If

$$I(\alpha) \equiv \int_0^\infty \Phi(\alpha y) \; e^{-\frac{1}{2}y^2\left(\frac{1-\rho^2}{\rho^2}\right)} dy, \tag{25}$$

then,

$$\frac{\delta I(\alpha)}{\delta \alpha} = \frac{-1}{\sqrt{2\pi}} \int_0^\infty y e^{-\frac{1}{2}\alpha^2 y^2} e^{-\frac{1}{2}y^2\left(\frac{1-\rho^2}{\rho^2}\right)} dy. \tag{26}$$

Substituting $x = \frac{y^2}{2}$,

$$I'(\alpha) = \frac{-1}{\sqrt{2\pi}} \int_0^\infty e^{-x\left(\alpha^2 + \left(\frac{1-\rho^2}{\rho^2}\right)\right)} dx \tag{27}$$

$$= \frac{1}{\sqrt{2\pi}\left(\alpha^2 + \left(\frac{1-\rho^2}{\rho^2}\right)\right)}. \tag{28}$$

Therefore,

$$I(\alpha) = \frac{\rho}{\sqrt{2\pi\left(1-\rho^2\right)}} \arctan\left(\frac{\alpha\rho}{\sqrt{1-\rho^2}}\right) + C. \tag{29}$$

To solve for C we utilize equation 25 with $\alpha = 0$,

$$I(0) = \int_0^\infty \frac{1}{2} e^{-\frac{1}{2}y^2\left(\frac{1-\rho^2}{\rho^2}\right)} dy. \tag{30}$$

Substituting $x = y\sqrt{\left(\frac{1-\rho^2}{\rho^2}\right)}$,

$$I(0) = \frac{\sqrt{2\pi}}{2\sqrt{\frac{1-\rho^2}{\rho^2}}} \int_0^\infty e^{-\frac{1}{2}x^2} dx \;\Rightarrow I(0) = \frac{\sqrt{2\pi}}{4\sqrt{\frac{1-\rho^2}{\rho^2}}}. \tag{31}$$

Equating equation 25 and equation 29 with $\alpha = 0$,

$$C = \frac{\sqrt{2\pi}}{4\sqrt{\frac{1-\rho^2}{\rho^2}}}. \tag{32}$$

The function $I(\alpha)$ becomes,

$$I(\alpha) = \frac{\rho}{\sqrt{2\pi}\,(1-\rho^2)} \arctan\left(\frac{\alpha\rho}{\sqrt{(1-\rho^2)}}\right) + \frac{\sqrt{2\pi}\rho}{4\sqrt{(1-\rho^2)}}. \tag{33}$$

Substituting equation 33 into equation 24,

$$P\left(X \geq 0, Y \geq 0\right) = \sqrt{D}\left[\frac{-1}{2\pi\sqrt{1-\rho^2}} \arctan\left(\frac{\rho}{\sqrt{1-\rho^2}}\right) - \frac{1}{4\sqrt{1-\rho^2}}\right]. \tag{34}$$

A similar procedure can be used with minor changes to find the second term in equation 17 which can be shown to be,

$$P\left(X \geq 0, Y < 0\right) = \sqrt{D}\left[\frac{-1}{2\pi\sqrt{1-\rho^2}} \arctan\left(\frac{\rho}{\sqrt{1-\rho^2}}\right) + \frac{1}{4\sqrt{1-\rho^2}}\right]. \tag{35}$$

Substituting equation 34 and equation 35 and D into equation 17, the expected value of Z_i is obtained,

$$\mathbb{E}\left[Z_i\right] = \frac{2}{\pi} \arctan\left(\frac{\rho}{\sqrt{(1-\rho^2)}}\right). \tag{36}$$

This expected value can be used to estimate both the correlation and the Hurst index. Solving equation 36 for ρ we obtain estimates,

$$\hat{\rho} = \frac{\tan\left(\frac{\pi}{2}E\left[Z_i\right]\right)}{\left[\tan^2\left(\frac{\pi}{2}E\left[Z_i\right]\right) + 1\right]^{\frac{1}{2}}}. \tag{37}$$

Since $\rho = 2^{2H-1} - 1$ then we obtain the ergodic "Quadrant method" estimator for H,

$$\hat{H} = \frac{\frac{\log(\hat{\rho}+1)}{\log(2)} + 1}{2}. \tag{38}$$

Computationally, this algorithm is very fast and fairly accurate (see §4 for numerical results). The major advantage of this method is that estimates are not largely affected by outliers, since the magnitude of the observed values does not disproportionately influence the estimator. This means the Quadrant method is robust to data that may not perfectly follow a fractional Wiener process, see §3.3. An ergodic estimator of H can also be derived using constant volume ellipsoids for the function $E\left[X_i X_{i+1}\right]$. The derivation of this statistic is very similar to the Quadrant method derivation, however it requires the use of a non-linear mixed integer optimization method.

3 Robustness of Hurst Index Estimators

The "Influence Curve" is a way to evaluate the sensitivity of an estimator to one contaminating point and therefore understand the "local robustness" of the estimators when the rest of the observations are assumed to come from the true distribution (Huber [6], pp.14); fGn is a Gaussian process with mean zero, variance $(\Delta t)^{2H}$ and covariance

$$\mathbb{E}[X_i X_j] = \frac{(\Delta t)^{2H}}{2}\left(|i-j+1|^{2H} + |i-j-1|^{2H} - 2|i-j|^{2H}\right)$$

where Δt is a known constant and $X_i = W^H_{i+1} - W^H_i$. In this section we create and compare influence curves for various estimators of the Hurst index. The influence curves $IC(x,H)$ are generated with contaminating values of $x = k(\Delta t)^H$, $k \in [-3,3]$ for $H = 0.1, \ldots, 0.9$. Since the true distribution of the data is assumed to be normally distributed, this is equivalent to the contaminating observation falling within an interval of three sigma. The graphs are all generated with $\Delta t = 1/252$ and a sample size $n = 156$, therefore we see the influence of the 157^{th} observation. A summary of the sensitivity of the Hurst estimators to a single contaminator $x = \pm 3(\Delta t)^H$ appears in Figure 2.

Figure 2:

Contaminator	H=0.1	H=0.2	H=0.3	H=0.4	H=0.5	H=0.6	H=0.7	H=0.8	H=0.9
2nd Moment Method									
$-3\Delta t^H$	-0.004	-0.004	-0.004	-0.004	-0.004	-0.004	-0.004	-0.004	-0.004
$+3\Delta t^H$	-0.004	-0.004	-0.004	-0.004	-0.004	-0.004	-0.004	-0.004	-0.004
Ratio Method									
$-3\Delta t^H$	0.036	0.027	0.018	0.011	0.005	-0.001	-0.006	-0.010	-0.014
$+3\Delta t^H$	0.036	0.027	0.018	0.011	0.005	-0.001	-0.006	-0.010	-0.014
Quadrant Method									
$-3\Delta t^H$	0.003	0.002	0.001	0.001	0.000	-0.001	-0.001	-0.001	-0.002
$+3\Delta t^H$	0.003	0.002	0.001	0.001	0.000	-0.001	-0.001	-0.001	-0.002
Whittle's Method									
$-3\Delta t^H$	0.055	0.029	0.014	0.005	0.000	-0.005	-0.009	-0.014	-0.027
$+3\Delta t^H$	0.060	0.032	0.017	0.007	0.001	-0.004	-0.009	-0.014	-0.027
Peng's Variance of Residuals Method									
$-3\Delta t^H$	0.073	0.046	0.026	0.012	0.003	-0.003	-0.007	-0.010	-0.012
$+3\Delta t^H$	0.077	0.049	0.029	0.015	0.006	-0.001	-0.005	-0.008	-0.010

3.1 Influence Curve for the Second Moment Method

In the Second Moment method estimator, the addition of one extra term, x, in the series causes a change to the estimation of the Hurst index of:

$$H_{n+1} = \frac{\log\left[\frac{n(\Delta t)^{2H_n}+x^2}{n+1}\right]}{2\log(\Delta t)} \tag{39}$$

This gives the empirical influence function

$$IC(x,H) = H_{n+1} - H_n = \frac{\log\left[\left(\frac{1}{n+1}\right)\left\{n + \frac{x^2}{(\Delta t)^{2H_n}}\right\}\right]}{2\log(\Delta t)}. \tag{40}$$

Figure 3:

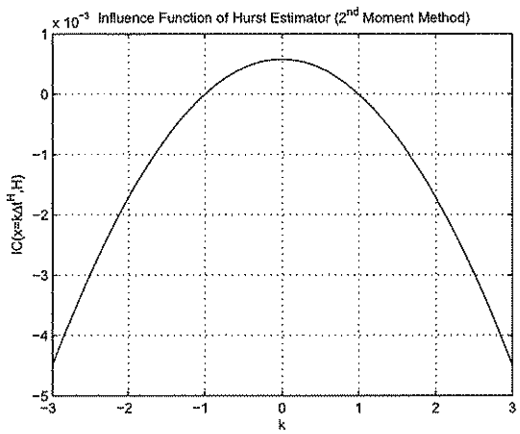

In Figure 3 we see that a contaminating point that is within three sigma of the true distribution has a maximum influence of $\pm 4x10^{-3}$ for all Hurst values. Given the scale, the influence curve for the Second Moment method is relatively flat over a $\pm 3\sigma$ range of values of x. Additionally, the maximum of the influence curve occurs at a height of $\log\left(\frac{n}{n+1}\right)/2\log(\Delta t) \geq 0$, $\Delta t < 1$.

3.2 Influence Curve for the Ergodic Ratio of Second Moments Method

The influence curve for the Ratio method estimator is similar to the Second Moment method in that it is a function of two Second Moments:

$$H_n = \frac{\log\left[\frac{SS_{2,n}}{SS_{1,n}}\right]}{2\log(2)}, \tag{41}$$

where

$$SS_{2,n} = \frac{\sum_{i=1}^{n-1}\left(X_{i+1}+X_i\right)^2}{n-1}$$

$$SS_{1,n} = \frac{\sum_{i=1}^{n}\left(X_i\right)^2}{n}.$$

Since the influence curve is derived assuming that none of the $\{X_i\}_{i=1}^n$ deviate from the true distribution, we know that $SS_{1,n} = \sigma^2\left(\Delta t\right)^{2H_n}$ and $SS_{2,n} = \sigma^2\left(2\Delta t\right)^{2H_n}$. Notice that $SS_{1,n}$ is the same as the ergodic Second Moment method, and therefore if we add one more term in the sequence, x, then we have

$$SS_{1,n+1} = \frac{nSS_{1,n}+x^2}{n+1}. \tag{42}$$

The term $SS_{2,n+1}$ is the same as the ergodic Second Moment method with half the sample rate, however to compute the influence of the contaminator, x, we need to consider the location of this extra observation. If the observation is at the beginning or the end of the sequence, it only affects the estimate in one term (notice in the formula for $S_{2,n}$ that the terms X_1 and X_n are only counted once, while all other X_i, $2 \le i \le n-1$ appear in two terms of $\left(X_{i+1}+X_i\right)^2$. Therefore, to see the maximum influence of an additional observation, we need to place the contaminating observation somewhere in between the first and last. Without loss of generality, we can place it right before the last observation, giving the sequence $\{X_1, X_{2,\ldots}, X_{n-1}, x, X_n\}$. Therefore,

$$SS_{2,n+1} = \frac{(n-2)SS_{2,n}+(x+X_{n-1})^2+(X_n+x)^2}{n}. \tag{43}$$

Since X_i and X_{i+1} come from the true distribution,

$$\mathbb{E}\left[(x+X_{n-1})^2+(X_n+x)^2\right] = 2\sigma^2\left(\Delta t\right)^{2H_n}+2x^2.$$

In this framework x is treated as a constant. Therefore, since the estimator

$$\mathbb{E}\left[SS_{2,n}\right] = \sigma^2(2\Delta t)^{2H_n},$$

the expected influence of x has the form:

$$IC(x,H) = \log\left[\left(\frac{n+1}{n}\right)\left(\frac{(n-2)\sigma^2(2\Delta t)^{2H_n} + 2\sigma^2(\Delta t)^{2H_n} + 2x^2}{n\sigma^2(\Delta t)^{2H_n} + x^2}\right)\right] / 2\log(2) - H_n. \tag{44}$$

When $\sigma^2 = 1$, then we obtain the influence curves in Figure 4.

Figure 4:

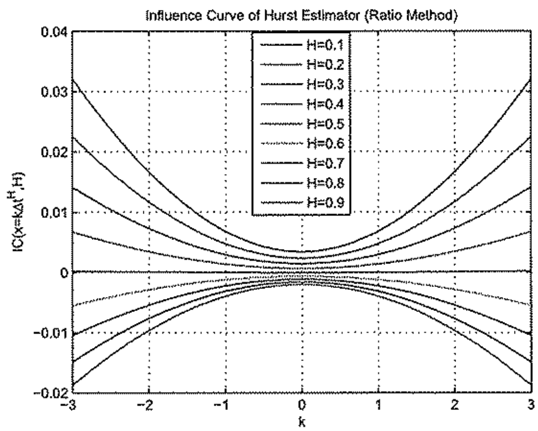

Figure 4 shows that the Ratio method's influence curve changes concavity when the process changes from long to short range dependence. The Ratio method has more sensitivity than the ergodic Second Moment for all Hurst values. The contaminating point's influence on the estimator increases as the Hurst index get further away from $H = 0.5$; more sensitivity occurs when the process has negative auto-correlation.

3.3 Influence Curve for the Ergodic Quadrant Method

Given the fractional Wiener process, $\{X_i\}_{i=1}^n$, the Hurst index estimator using the Quadrant method is a function of the statistic

$$T_n = \frac{\sum_{i=1}^{n-1} sgn(X_i)sgn(X_{i+1})}{n-1}. \tag{45}$$

The correlation of normals is then estimated by

$$\rho_n = \frac{\tan(\frac{\pi}{2}T_n)}{\sqrt{\tan(\frac{\pi}{2}T_n)^2 + 1}}. \tag{46}$$

Lastly, the Hurst index is computed

$$H_n = \frac{\left(\frac{\log(2\rho_n+2)}{\log(2)}\right)}{2}. \tag{47}$$

In order to compute the influence curve, we need to understand the estimator T. Once again to get the maximum contribution of an additional observation, we need to place the observation between the first and last X_i. If we place the contaminating data point, x, in the sequence as before $\{X_1, X_{2,\ldots,} X_{n-1}, x, X_n\}$:

$$T_{n+1} = \frac{(n-1)T_n + sgn(X_{n-1})sgn(x) + sgn(x)sgn(X_n)}{n} \tag{48}$$

The property of the signum function yields only three results, none of which are dependent on the magnitude of the contaminant, but only on the sign of the new observation and the sign of the immediately adjacent observations. This is because the Quadrant method attempts to find momentum in the time series. The function, T, looks for long term tendencies of the time series in a particular direction. The different outcomes are given in the following matrix.

$sgn(X_{n-1})sgn(x) + sgn(x)sgn(X_n)$	$x \geq 0$	$x < 0$
$X_i \geq 0, X_{i+1} \geq 0$	$1+1=2$	$-1-1=-2$
$X_i \geq 0, X_{i+1} < 0$	$1-1=0$	$-1+1=0$
$X_i < 0, X_{i+1} \geq 0$	$-1+1=0$	$1-1=0$
$X_i < 0, X_{i+1} < 0$	$-1-1=-2$	$1+1=2$

Therefore,

$$T_{n+1} = \begin{cases} \frac{(n-1)T_n - 2}{n} & \text{with probability } \frac{1}{4} \\ \frac{(n-1)T_n}{n} & \text{with probability } \frac{1}{2} \\ \frac{(n-1)T_n + 2}{n} & \text{with probability } \frac{1}{4} \end{cases} . \tag{49}$$

If all observations came from the true distribution, then

$$\mathbb{E}[T] = \frac{2}{\pi} Arctan\left(\frac{2^{2H-1}-1}{\sqrt{1-(2^{2H-1}-1)^2}}\right). \tag{50}$$

Therefore we can substitute the true statistic $\mathbb{E}[T]$ for T_n to show the expected influence of the contaminating term, x, on H_{n+1}. Performing this substitution, the influence curve can either be constant (when the contaminating point adds zero to the estimate of T_{n+1}) or the curve is $\pm$ a constant, with jumps left and right of the center (when the contaminating point adds $\pm 2/(n+1)$ to the estimate of T_{n+1}).

Figure 5:

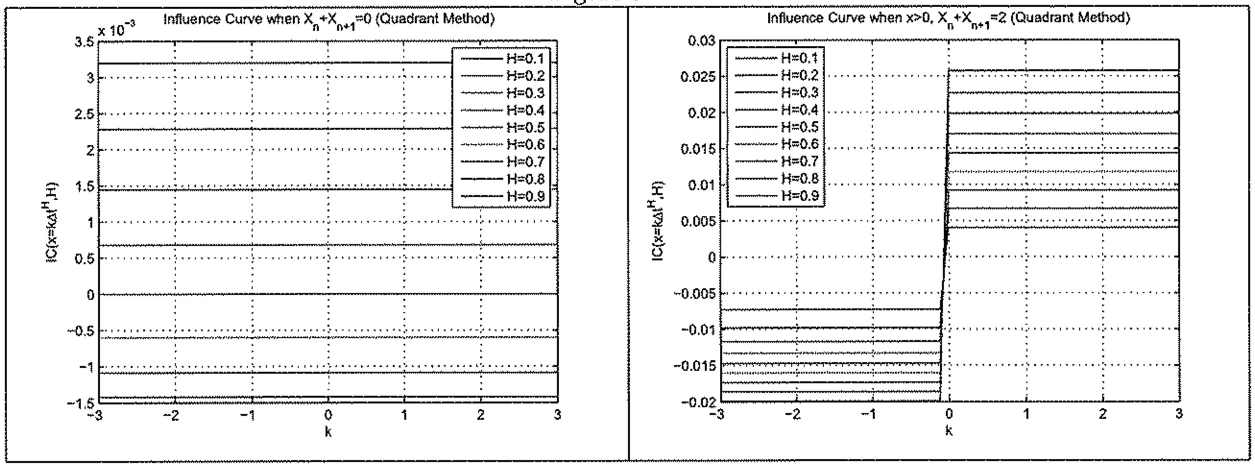

Note that the right graph in Figure 5 will always have an influence curve that jumps in the same pattern, (down on one side and up on the other or vise-versa). The jump pattern depends on the sign of the observations immediately adjacent to the contaminating point x. The analysis above shows that the short range dependent process $\left(H < \frac{1}{2}\right)$ has much more sensitivity to the contaminating observation than the long-memory process $\left(H > \frac{1}{2}\right)$.

Figure 6:

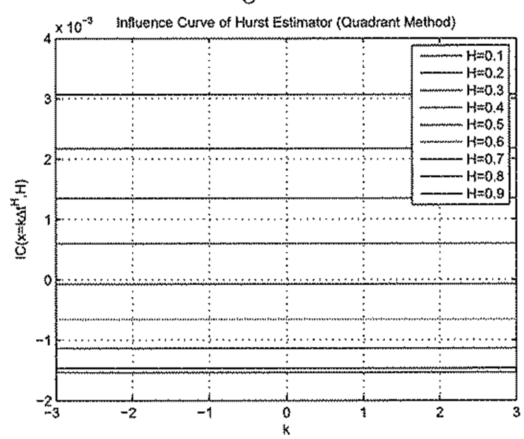

In figure 6 we can see the expected influence curve for the Quadrant method's Hurst index estimator shows the extreme robustness to the size of the contaminating point. The Quadrant method is the most robust method discussed in this paper.

3.4 Influence Curve for the Whittle's Approximate MLE and Peng's Variance of Residuals

Whittle's approximate MLE is calculated by minimizing the log ratio of the Periodogram (calculated from data) and the theoretical Spectral density function for fGn. The computation of the Spectral density function for fGn requires a truncated infinite sum (or linear approximation). Additionally, to calculate the estimates of the Hurst index, we need to numerically optimize a convex objective function. Whittle's objective function gives an estimator of the variance affecting the process, $\sigma^2(\Delta t)^{2H}$, at the optimal solution. This is accomplished using the Golden Section method.

To compute the influence curve we need to understand the influence curve of the Periodogram, which coupled with the optimization over the spectral density, complicates this calculation to an intractable degree since it is necessary to compute the contribution of the contaminant, x, for all $n/2$ Fourier frequencies. We have to resort to another way to evaluate the influence of x. One way to generate the influence curve is to use Monte-Carlo simulation.

Figure 7:

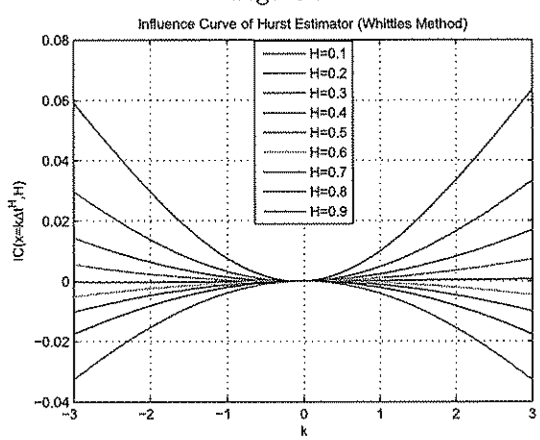

In Figure 7 we can see the average influence curve for Whittle's method. These curves were generated by simulating 500 replications of fractional Gaussian generated noise using the Durbin-Levinson algorithm with $N = 156$ observations. The Hurst index was then estimated via Whittle's algorithm, then the observation x was placed at position $n/4$. This created another sample with $n = 157$ observations, which was used to estimate the Hurst index for the same x values used in the ergodic estimator influence curves. The estimated value of H_n for each replication was then subtracted from the estimate H_{n+1}, giving the influence curve. These 500 replications for each $H = 0.1, \dots, 0.9$ were then averaged for each value of x to produce the average influence curves above. Whittle's method does not appear to be locally robust for $H < \frac{1}{2}$, while it is more robust when $H \geq \frac{1}{2}$. While there does not seem to be any literature on the influence curve of Whittle's method, Taqqu [13] on page 724 recognizes that

> "it is a parametric model in that it assumes the spectral density of the series is know with the exception of a few parameters, which are to be estimated. This assumption allows for very precise estimation when the series being examined fits the assumed model exactly. If, on the other hand, the actual series is not of the exact form specified in the model, the parametric estimators may give incorrect results."

In his paper, Taqqu discusses different techniques that have been developed to robustify Whittle's Approximate MLE. One such technique smooths out the higher frequencies in the data. The noise typically present in real data occurs at higher frequencies. This noise can skew values spectral density function, resulting in a biased Hurst index estimate. The fact that there are at least four different methods that have been developed to robustify Whittle's MLE, indicates that this estimator may not be robust enough for certain real data sets. Taqqu [13] shows how each one of these robustified Whittle estimators changes for a given set of Ethernet data. Our simulations indicated that on average, a given contaminating point results in slightly worse deviations in Whittle's Approximate MLE than the ergodic Ratio method for all Hurst index values except $H = 0.3, 0.4$ and 0.5.

Peng's Variance of Residuals method estimates the Hurst index from the errors of a linear regression on a log of aggregated variance calculations. We perform a Monte-Carlo simulation in the same fashion as in the influence curve for Whittle's estimator.

Figure 8:

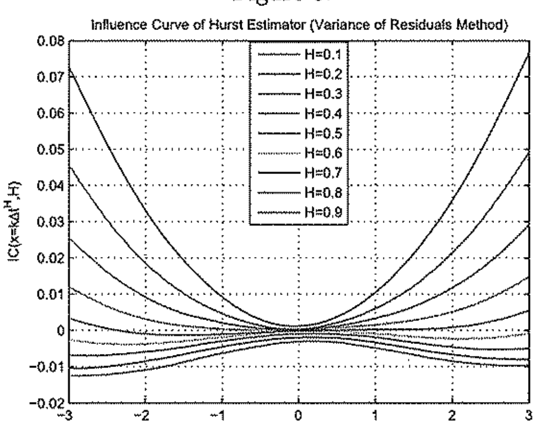

In Figure 8 we can see the average influence curve for Peng's Variance of Residuals method. Notice that this method is more robust (on average) to a single contaminating value when $H \geq \frac{1}{2}$. Its influence curve for these Hurst values is comparable to the Ratio method's influence curve. When $H < \frac{1}{2}$, this method is the least robust (on average) out of the estimators presented in this paper.

4 Numerical Results for Simulations

In this section, we compare via Monte Carlo simulation, the performance of the newly introduced ergodic estimators of the Hurst index to Whittle's approximate MLE and Peng's Variance of Residuals estimators. Taqqu et al. [11] presents an empirical study of many estimators of the Hurst index in the same fashion. They show empirically that Whittle's approximate MLE estimator is the best estimator (of those tested) in terms of RMSE for a fBm time series. Their study indicates that Peng's Variance of Residuals method is the second best of the methods tested.

Taqqu generated 50 sample paths of fGn each with a sample size of $N = 10,000$ for $H = 0.5, 0.6, 0.7, 0.8, 0.9$ using Monte Carlo simulation (Durbin-Levinson algorithm). He computed the sample mean, sample variance and RMSE of the Hurst index estimators for each technique. Using the Durbin Levinson algorithm, we simulate 500 sample paths of fGn with length $N = 10,000$ and $\Delta t = 1/252$. We extend the analysis for processes with both short range ($H < 1/2$) and long range dependence ($H > 1/2$) by simulating $H = 0.1, 0.2, \ldots, 0.9$ using Matlab®. For each $H = 0.1, 0.2, \ldots, 0.9$ we used the method of common random numbers with the same seed to generate 500 x 10,000 i.i.d. standard normal random variates for each set of paths. We increased the number of sample paths (compared to Taqqu et al. [11]) in order to increase the accuracy of our estimates of Root Mean Square Error (RMSE) and allow for the identification of significant differences in the estimators (see §4.2).

We implemented Whittle's algorithm using the spectral density approximation described by Ledesma and Liu [7], and use $n = 500$ terms in the linear approximation of the spectral density at each Fourier frequency. We found that even though Ledesma and Liu recommend $n = 200$ terms, at least $n = 500$ terms are needed in the linear approximation are needed due to of the slow convergence rate of the spectral density when $H \in (0, 0.3)$. Ledesma's recommendation was for $H \geq 1/2$. A Golden Section search algorithm is used to find the global maximum of Whittle's approximate MLE with a termination tolerance of 10^{-6} for the accuracy of the Hurst index estimate. The Golden Section method is initialized to search for the optimum on $H \in [0, 1]$. The ergodic algorithms do not require optimization and therefore are not constrained numerically on $H \in [0, 1]$. Peng's Variance of Residuals method is implemented for a minimum of 50 block sizes. Regression is performed on block sizes between $\left[10^{0.5}, 10^{0.7}\right]$. The median of residuals at each block size is used in the Hurst index estimator.

All computations were done using a Dell Optiplex 755 running Windows 7 with a 2.66 GHz Intel Core 2 Duo and 3326MB of RAM . The total time to compute all 4500 (500 paths by 9 Hurst index values) estimates of the Hurst index for different sample sizes are shown in Figure 9.

Figure 9:

	Run Time(s)					
	Whittle		Variance	Ergodic	Ergodic	Ergodic
N	tol=10^{-6}, n=500	tol=10^{-4}, n=200	Residuals	2nd Moment	Ratio	Quadrant
39	152.0	51.6	12.4	0.000	0.000	0.000
78	158.8	57.4	38.7	0.000	0.016	0.000
156	176.1	72.5	88.2	0.016	0.016	0.015
312	222.2	114.3	93.0	0.016	0.124	0.093
625	367.0	249.5	110.8	0.047	0.234	0.156
1250	855.7	719.2	253.6	0.109	0.468	0.344
2500	2658.7	2477.8	464.4	0.218	0.952	0.671
5000	9307.5	9100.1	1055.9	0.421	1.841	1.342
10000	35771.0	35559.6	1879.6	0.889	3.837	2.683

The power of closed-form representation of the ergodic estimators of the Hurst index can be seen by the magnitude of difference in computational time for all nine simulations; ergodic estimators take seconds or less while for large data sets Whittle's approximate MLE can take tens of hours. Whittle's lengthy computational time is primarily due to the re-computation of the spectral density function for each iteration of H in the optimization algorithm. Simple algorithms like the Variance of Residuals method can also be seen to take significantly more computational time than the ergodic methods.

4.1 Empirical Performance of Estimators

In this section we analyze the behavior of the estimators as the length of the fBm time-series is reduced, giving insight into the convergence rate. Difference analysis is used to demonstrate which estimators are more accurate. We provide a comparison of the various estimators for the 500 sample paths of fractional Brownian motion. Appendix I shows comparisons of the Hurst index estimators from the 500 x 9 simulated fBm paths via box-plots. The boxes represent the inter-quartile range (75 percent of the estimates fall in this range). The lines inside the boxes indicate the mean of the non-outlier points. The plus signs show outlier points, which are defined by values greater than the 'whiskers' length which is 1.5 times the distance outside the inter-quartile range.

Figure 10:

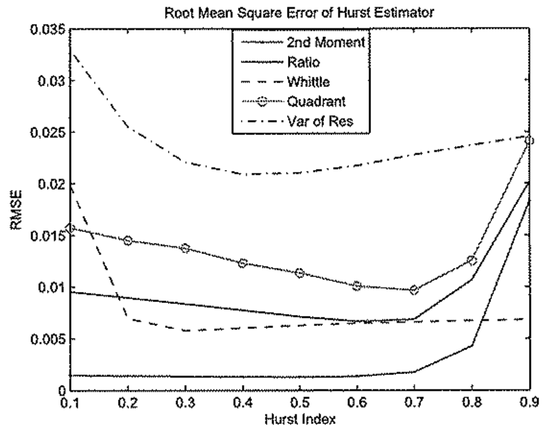

Figure 10 shows a comparison of each method for $N = 10,000$ data points in each time-series. In Appendix III, we provide a breakdown of the sample bias $\left(Bias(H,\hat{H}) = mean\left(\hat{H} - H\right)\right)$ and sample variance of the estimators since

$$RMSE(\hat{H}) = \sqrt{Var(\hat{H}) + (Bias(H,\hat{H}))^2}. \tag{51}$$

The ergodic estimators have similar performance to each other in that they have little bias for $H \in [0.1, 0.8]$ and increased bias for H values closer to 0.9. The ergodic estimates have the least standard deviation for $H \in [0.5, 0.7]$ and higher deviation as $H \to 1$. On the other hand, the Whittle estimates seem to underestimate the Hurst index on average, with more error as $H \to 0$. This is due to the slow convergence rate of the spectral density function. If the linear approximation of the spectral density is changed to include more terms, the accuracy of the estimators at $H = 0.1$ will improve slightly because of the slow convergence rate of the spectral density function, however this comes at the cost of computational time. We found that as $H \to 0$, the number of terms needed in the approximation of the spectral density explodes. However, setting $n = 500$ or more seems to have little affect on the convergence of the Hurst estimators when $H \geq 0.2$. Whittle's standard deviation increases as H becomes larger.

The simulation results show that the ergodic estimates are less biased for all values of H when compared to Whittle's estimates. It should be noted that while the Second moment method shows superior performance to all other methods, it assumes that the drift and scale affecting the fBm process are known. The other methods do not require this information to estimate the Hurst index. In the other methods the drift $\mu = 0$ and a scale $\sigma = 1$. These paramters are assumed to be unknown in the estimation of the Hurst index. The Quadrant method gives accurate estimates, however they are not as accurate as the Ratio method.

In the next sub-section we will see that the Quadrant method outperforms the Variance of Residuals method for almost all sample sizes and almost all Hurst index values, however it is not as accurate as Whittle's approximate MLE. We also demonstrate that the Ratio method is comparable to Whittle's approximate MLE on smaller sample sizes for central values of the Hurst index.

4.2 Difference Analysis and Numerical Convergence of Hurst Index Estimators

We use the various estimators discussed in this paper to estimate the Hurst index on the simulated paths of fGn and then compare the estimator's absolute deviation using the paired t-test. If we let,

$$D = average\left[\left|\hat{H}_1 - H_{Actual}\right| - \left|\hat{H}_2 - H_{Actual}\right|\right] \tag{52}$$

$$\sigma_D^2 = Var\left[\left|\hat{H}_1 - H_{Actual}\right| - \left|\hat{H}_2 - H_{Actual}\right|\right] \tag{53}$$

The confidence interval on the statistic D can be shown to be approximately,

$$D \pm \sigma_D t_{\frac{\alpha}{2},N-1}. \tag{54}$$

We use equation 54 to construct 99% confidence interval for testing the null hypothesis

$$\begin{aligned} H_0 &: \left|\hat{H}_1 - H\right| = \left|\hat{H}_2 - H\right| \\ H_1 &: \left|\hat{H}_1 - H\right| \neq \left|\hat{H}_2 - H\right| \end{aligned}$$

The results of the analysis can be seen below in Figure 11. The inclusion of zero in the confidence interval indicates that there is no significant difference in the estimators.

Figure 11:

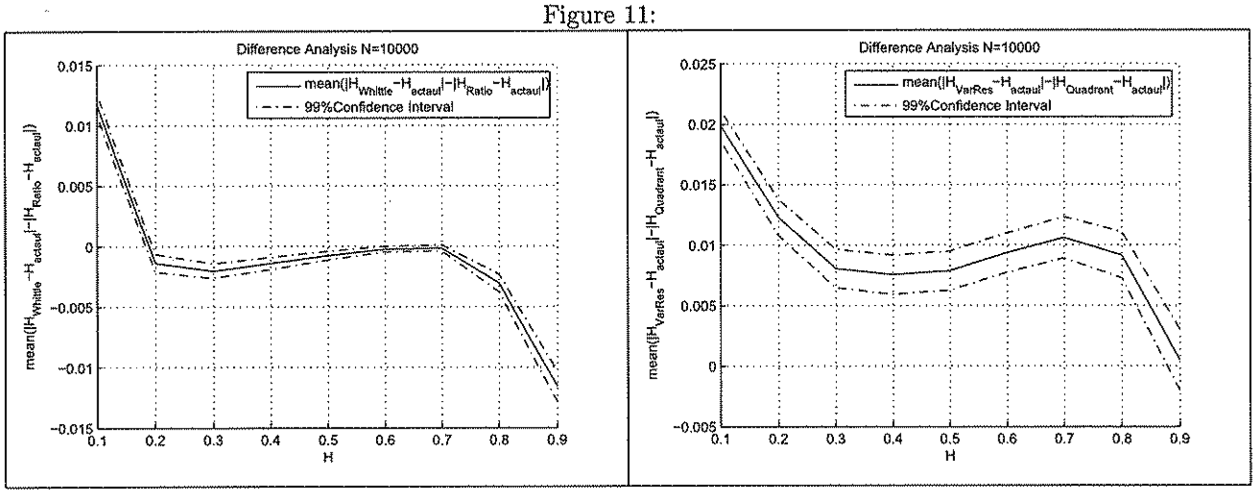

The analysis in Figure 11 (left) indicates for $N = 10,000$ that the Ratio method's estimates of H are significantly better than Whittle's estimates on average when $H = 0.1$, and that there is no significant difference between the estimators for $H = 0.6, 0.7$. Whittle's approximate MLE's estimates are slightly better than the Ratio's estimates for the H values between 0.2 and 0.6 and significantly better for 0.8 and 0.9. Furthermore in Figure 11 (right), the Quadrant method is shown to be statistically significantly more accurate than the Variance of Residuals method for all Hurst index values except for $H = 0.9$, where there is no statistical difference. The superiority of the Quadrant method when compared to the Variance of Residuals method is fairly consistent as sample size is decreased (see Appendix II). In Figure 12, the difference analysis is expanded to estimates when the sample size (N) is reduced for the Ratio and Whittle estimators.

Figure 12:

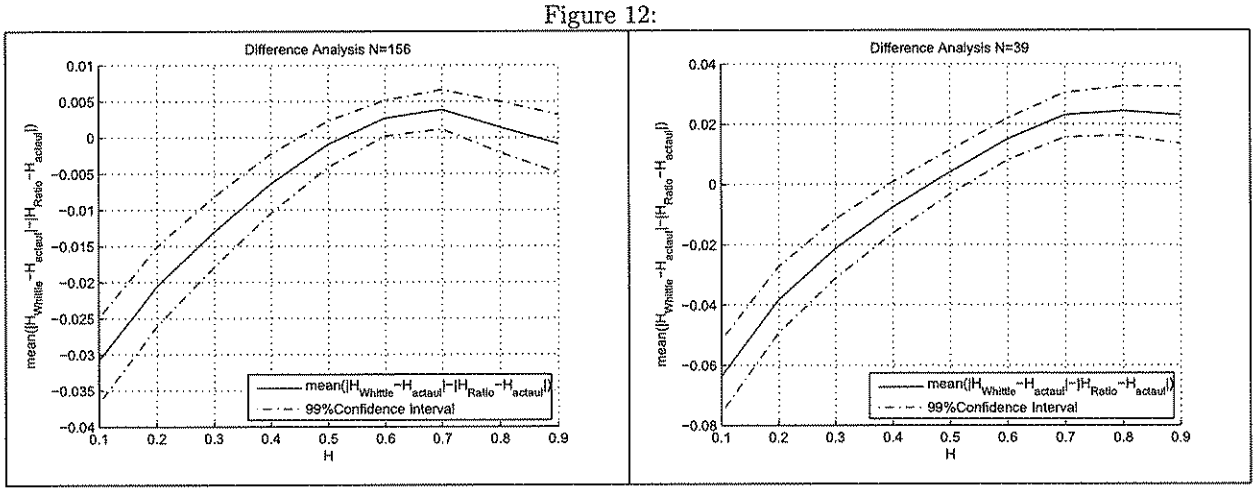

Figure 12 shows the difference analysis for Whittle and Ratio method sample paths with $N = 156$ (left) and 39 (right). The analysis indicates that the Ratio method produces more accurate estimates on average for H (in terms of RMSE) than Whittle's method for $H > 0.6$ and equivalent for $H = 0.5$ when $N = 39$ and 156. When N is increased to $N = 625$, the Ratio method still yields estimates that are not significantly different than Whittle's estimates for values of $H = 0.6, 0.7$ and 0.8. It is not until $N = 1,250$ that Ratio performs similarly to Figure 11 and falls behind Whittle's approximate MLE. Full details of the difference analysis can be found in Appendix II. The results in Appendix II have also be confirmed via the Wilcoxon signed-rank test.

The superior performance of the ergodic estimators for small sample size is a result of the convergence rate of the estimators. Whittle's approximate MLE converges at a rate of $\sqrt{N}$ (Taqqu et al. [13]) . Figure 13 provides a simulation based comparison of the numerical convergence rates of the RMSE.

Figure 13:

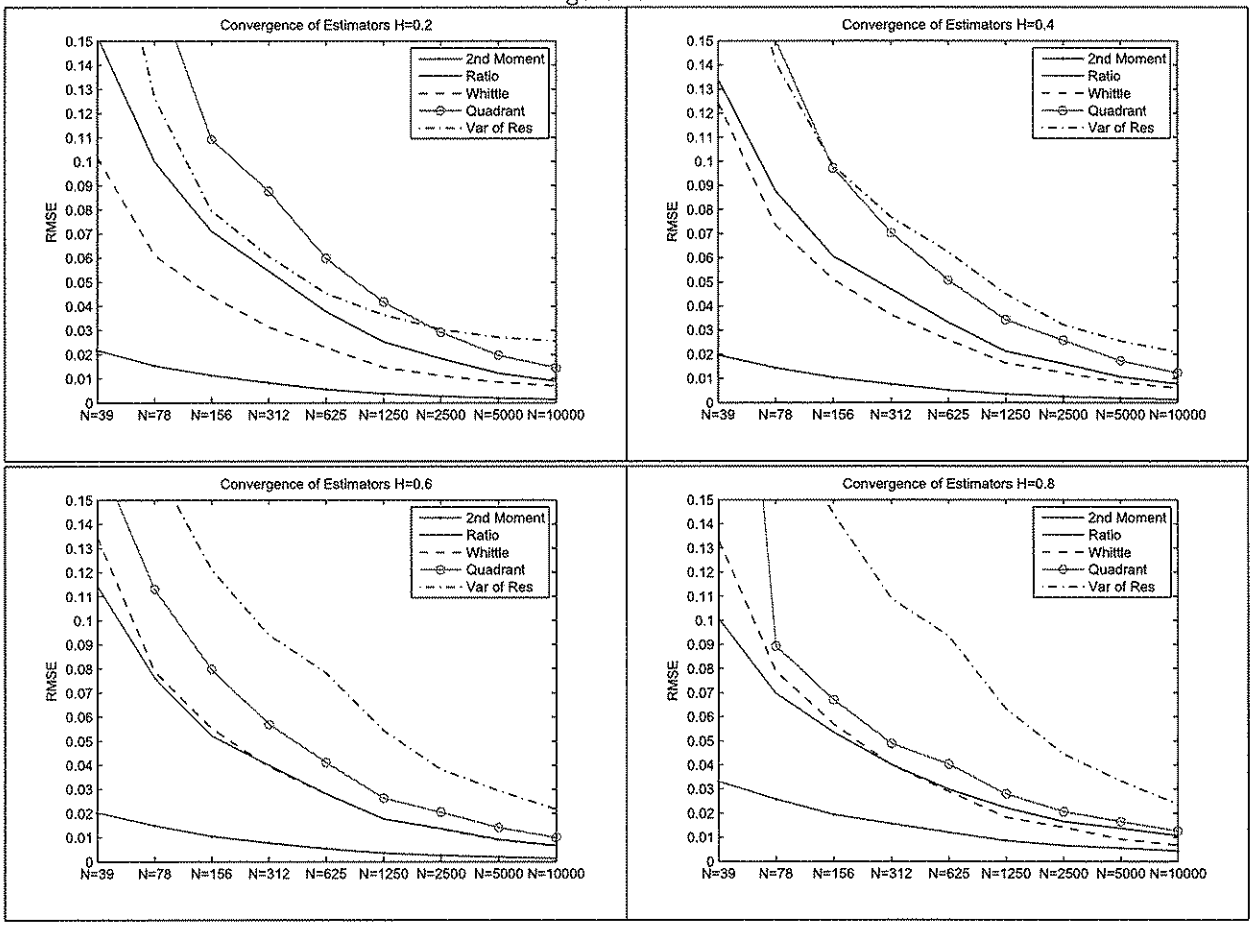

Figure 13 (above) compares the convergence rates for selected H values. Notice that the Ratio method performs similar to Whittle, while the Quadrant method requires $N > 78$ when $H \geq 0.8$. Full details can be found in Appendix III. Notice that the convergence rate for highly auto-correlated processes ($H = 0.2$ and$H = 0.8$) are significantly slower for the ergodic methods. The Ratio method performs similarly to Whittle's method for $H = 0.6$ and 0.7.

5 Conclusion

In this paper we have introduced three new methods of estimating the Hurst index using ergodic theory. These methods have been shown to be comparable in performance to leading estimators in terms of RMSE. Our empirical analysis shows the robustness and computational speed of the ergodic estimators. The Second Moment method can be used for estimating the Hurst index when there is known location and scale. This method has been shown to be equivalent to or more accurate than Whittle's approximate MLE with a computational speed 10^4 faster due to its simplicity. We have shown that the Ratio and Quadrant methods are consistent and competitive estimators of the Hurst index for fractional Wiener processes. The Ratio method becomes comparable to Whittle's estimator for $H \geq 1/2$ index for small sample sets ($N \leq 156$ data points), while the Quadrant method is robust and still outperforms most methods available. All methods introduced are statistically equivalent to or better than Peng's Variance of Residuals method (for most values of the Hurst index), the second best method reported in Taqqu et al. [11].

The primary advantage of the ergodic estimators introduced in this paper is the availability of a closed-form solution for estimating the Hurst index. Methods like Whittle's approximate MLE require optimization algorithms which can take significant time to calculate. Simpler methods sacrifice accuracy for speed. The ergodic Ratio and Second Moment estimators have speed and simplicity with little sacrifice of accuracy. Additionally, the ergodic estimators show superior relative performance on small sample sizes. These properties are important in such fields as finance (Willinger et al. [15]) and network flow, where fractional Brownian motion models are being used, and reliable and fast estimates of the Hurst index are needed for decision making using small sample sizes.

Appendix I

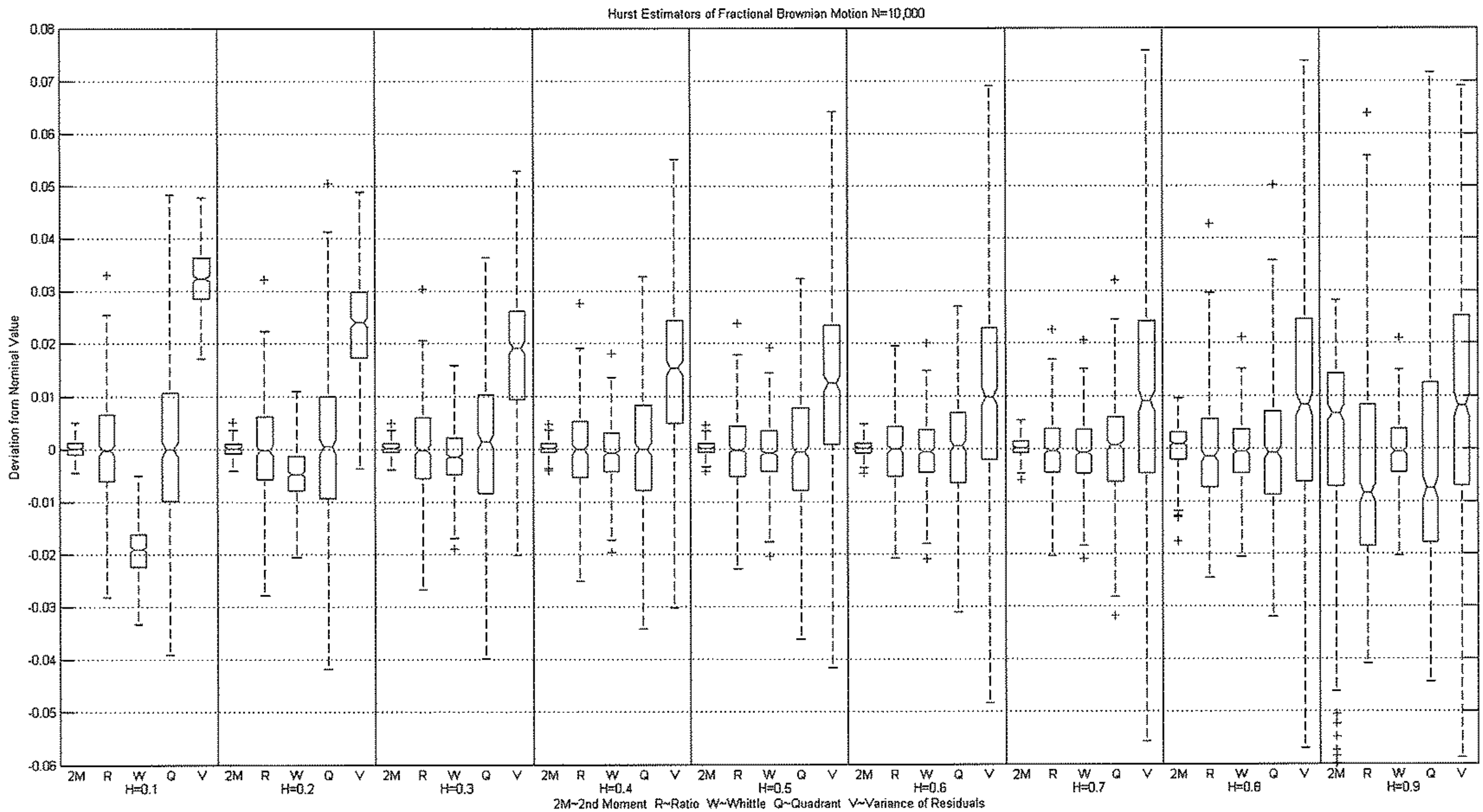
Hurst Estimators of Fractional Brownian Motion N=10,000
Deviation from Nominal Value
0.08
0.07
0.06
0.05
0.04
0.03
0.02
0.01
0
-0.01
-0.02
-0.03
-0.04
-0.05
-0.06
2M R W Q V
H=0.1
H=0.2
H=0.3
H=0.4
H=0.5
H=0.6
H=0.7
H=0.8
H=0.9
2M~2nd Moment R~Ratio W~Whittle Q~Quadrant V~Variance of Residuals

Appendix II

Difference Analysis

Whittle vs Ratio — Ratio Method Significantly Better Estimator | Statistically Equivalent Estimators | 99% Confidence Interval

N	H=0.1	H=0.2	H=0.3	H=0.4	H=0.5
10000	0.0117 (0.0108, 0.0126)	-0.0014 (-0.0021, -0.0006)	-0.0020 (-0.0026, -0.0014)	-0.0014 (-0.0019, -0.0009)	-0.0008 (-0.0011, -0.0004)
5000	0.0083 (0.0071, 0.0095)	-0.0029 (-0.0038, -0.0020)	-0.0028 (-0.0036, -0.0020)	-0.0018 (-0.0025, -0.0012)	-0.0008 (-0.0013, -0.0003)
2500	0.0042 (0.0031, 0.0054)	-0.0056 (-0.0070, -0.0043)	-0.0046 (-0.0057, -0.0035)	-0.0031 (-0.0040, -0.0021)	-0.0016 (-0.0023, -0.0009)
1250	-0.0043 (-0.0066, -0.0020)	-0.0086 (-0.0105, -0.0066)	-0.0065 (-0.0082, -0.0048)	-0.0041 (-0.0055, -0.0027)	-0.0018 (-0.0028, -0.0007)
625	-0.0107 (-0.0139, -0.0074)	-0.0124 (-0.0150, -0.0097)	-0.0093 (-0.0116, -0.0071)	-0.0061 (-0.0080, -0.0042)	-0.0030 (-0.0044, -0.0015)
312	-0.0246 (-0.0288, -0.0204)	-0.0196 (-0.0233, -0.0158)	-0.0142 (-0.0174, -0.0109)	-0.0092 (-0.0118, -0.0065)	-0.0047 (-0.0067, -0.0026)
156	-0.0308 (-0.0367, -0.0249)	-0.0206 (-0.0261, -0.0151)	-0.0131 (-0.0179, -0.0082)	-0.0064 (-0.0105, -0.0023)	-0.0009 (-0.0041, 0.0023)
78	-0.0463 (-0.0542, -0.0385)	-0.0306 (-0.0378, -0.0233)	-0.0206 (-0.0269, -0.0143)	-0.0120 (-0.0172, -0.0067)	-0.0041 (-0.0083, 0.0001)
39	-0.0636 (-0.0758, -0.0515)	-0.0382 (-0.0492, -0.0273)	-0.0213 (-0.0311, -0.0115)	-0.0077 (-0.0162, 0.0008)	0.0041 (-0.0032, 0.0114)

N	H=0.6	H=0.7	H=0.8	H=0.9
10000	-0.0002 (-0.0004, 0.0000)	-0.0001 (-0.0004, 0.0001)	-0.0030 (-0.0038, -0.0023)	-0.0116 (-0.0129, -0.0103)
5000	-0.0001 (-0.0004, 0.0002)	-0.0003 (-0.0006, 0.0001)	-0.0033 (-0.0042, -0.0023)	-0.0120 (-0.0135, -0.0104)
2500	-0.0003 (-0.0007, 0.0001)	0.0003 (-0.0002, 0.0007)	-0.0020 (-0.0032, -0.0007)	-0.0101 (-0.0120, -0.0082)
1250	0.0001 (-0.0006, 0.0008)	0.0004 (-0.0003, 0.0011)	-0.0031 (-0.0046, -0.0017)	-0.0119 (-0.0140, -0.0097)
625	-0.0002 (-0.0012, 0.0008)	0.0014 (0.0002, 0.0026)	0.0001 (-0.0021, 0.0024)	-0.0069 (-0.0096, -0.0042)
312	-0.0009 (-0.0024, 0.0006)	0.0010 (-0.0007, 0.0027)	-0.0002 (-0.0030, 0.0025)	-0.0072 (-0.0104, -0.0040)
156	0.0027 (0.0002, 0.0052)	0.0039 (0.0012, 0.0065)	0.0015 (-0.0021, 0.0050)	-0.0008 (-0.0049, 0.0032)
78	0.0022 (-0.0014, 0.0059)	0.0066 (0.0025, 0.0107)	0.0071 (0.0023, 0.0119)	0.0052 (-0.0005, 0.0109)
39	0.0150 (0.0081, 0.0219)	0.0231 (0.0156, 0.0305)	0.0245 (0.0163, 0.0326)	0.0231 (0.0136, 0.0325)

Variance of Residuals vs Quadrant — Quadrant Significantly Better Estimator | Statistically Equivalent Estimators | 99% Confidence Interval

N	H=0.1	H=0.2	H=0.3	H=0.4	H=0.5
10000	0.0199 (0.0187, 0.0212)	0.0123 (0.0108, 0.0138)	0.0081 (0.0065, 0.0097)	0.0076 (0.0060, 0.0092)	0.0079 (0.0063, 0.0095)
5000	0.0159 (0.0142, 0.0175)	0.0087 (0.0067, 0.0106)	0.0063 (0.0042, 0.0084)	0.0060 (0.0038, 0.0083)	0.0086 (0.0064, 0.0109)
2500	0.0083 (0.0059, 0.0108)	0.0028 (0.0001, 0.0056)	0.0026 (-0.0002, 0.0055)	0.0049 (0.0020, 0.0078)	0.0093 (0.0063, 0.0122)
1250	-0.0023 (-0.0059, 0.0014)	-0.0043 (-0.0080, -0.0006)	0.0014 (-0.0025, 0.0053)	0.0090 (0.0051, 0.0129)	0.0168 (0.0128, 0.0208)
625	-0.0156 (-0.0205, -0.0106)	-0.0123 (-0.0178, -0.0068)	-0.0037 (-0.0093, 0.0018)	0.0092 (0.0034, 0.0151)	0.0192 (0.0134, 0.0251)
312	-0.0228 (-0.0296, -0.0159)	-0.0208 (-0.0281, -0.0135)	-0.0109 (-0.0181, -0.0038)	0.0050 (-0.0023, 0.0124)	0.0153 (0.0078, 0.0227)
156	-0.0218 (-0.0317, -0.0119)	-0.0228 (-0.0325, -0.0132)	-0.0118 (-0.0218, -0.0019)	0.0025 (-0.0076, 0.0127)	0.0173 (0.0072, 0.0274)
78	-0.0352 (-0.0508, -0.0195)	-0.0313 (-0.0468, -0.0158)	-0.0181 (-0.0333, -0.0030)	-0.0031 (-0.0185, 0.0123)	0.0189 (0.0038, 0.0340)
39	-0.0204 (-0.0468, 0.0059)	-0.0132 (-0.0402, 0.0138)	0.0052 (-0.0192, 0.0296)	0.0143 (-0.0094, 0.0380)	0.0481 (0.0258, 0.0705)

N	H=0.6	H=0.7	H=0.8	H=0.9
10000	0.0094 (0.0077, 0.0110)	0.0106 (0.0089, 0.0123)	0.0092 (0.0073, 0.0111)	0.0005 (-0.0020, 0.0030)
5000	0.0115 (0.0092, 0.0138)	0.0134 (0.0110, 0.0158)	0.0135 (0.0108, 0.0161)	0.0056 (0.0023, 0.0089)
2500	0.0135 (0.0103, 0.0166)	0.0176 (0.0143, 0.0209)	0.0184 (0.0149, 0.0220)	0.0126 (0.0085, 0.0168)
1250	0.0227 (0.0185, 0.0269)	0.0274 (0.0230, 0.0317)	0.0295 (0.0247, 0.0343)	0.0246 (0.0192, 0.0300)
625	0.0296 (0.0235, 0.0357)	0.0365 (0.0303, 0.0428)	0.0433 (0.0365, 0.0501)	0.0454 (0.0378, 0.0530)
312	0.0287 (0.0209, 0.0364)	0.0405 (0.0326, 0.0484)	0.0486 (0.0404, 0.0568)	0.0504 (0.0413, 0.0595)
156	0.0339 (0.0239, 0.0440)	0.0499 (0.0396, 0.0602)	0.0628 (0.0519, 0.0736)	0.0696 (0.0580, 0.0812)
78	0.0405 (0.0265, 0.0545)	0.0597 (0.0456, 0.0737)	0.0733 (0.0589, 0.0876)	-0.0026 (-0.0918, 0.0866)
39	0.0683 (0.0469, 0.0897)	0.0979 (0.0763, 0.1196)	0.0995 (0.0547, 0.1443)	-0.1892 (-0.3421, -0.0363)

Appendix III

Estimated Root Mean Square Error **Paths=500**

Technique	H=0.1	H=0.2	H=0.3	H=0.4	H=0.5	H=0.6	H=0.7	H=0.8	H=0.9
N=10,000									
Var of Res	0.033	0.026	0.022	0.021	0.021	0.022	0.023	0.024	0.025
Whittle	0.020	0.007	0.006	0.006	0.006	0.006	0.007	0.007	0.007
Second Moment	0.001	0.001	0.001	0.001	0.001	0.001	0.002	0.004	0.018
Ratio	0.010	0.009	0.008	0.008	0.007	0.007	0.007	0.011	0.020
Quadrant	0.016	0.015	0.014	0.012	0.011	0.010	0.010	0.013	0.024
N=5,000									
Var of Res	0.034	0.027	0.025	0.026	0.027	0.029	0.031	0.033	0.035
Whittle	0.020	0.009	0.008	0.008	0.009	0.009	0.009	0.009	0.009
Second Moment	0.002	0.002	0.002	0.002	0.002	0.002	0.002	0.006	0.021
Ratio	0.013	0.012	0.012	0.011	0.010	0.009	0.009	0.014	0.023
Quadrant	0.021	0.020	0.018	0.017	0.015	0.014	0.014	0.016	0.028
N=2,500									
Var of Res	0.035	0.030	0.030	0.032	0.035	0.038	0.041	0.045	0.047
Whittle	0.020	0.011	0.012	0.012	0.013	0.013	0.014	0.014	0.014
Second Moment	0.003	0.003	0.003	0.002	0.002	0.003	0.003	0.007	0.021
Ratio	0.019	0.018	0.017	0.016	0.015	0.014	0.013	0.017	0.026
Quadrant	0.031	0.029	0.028	0.026	0.023	0.021	0.019	0.021	0.030
N=1,250									
Var of Res	0.037	0.036	0.040	0.045	0.050	0.054	0.059	0.063	0.068
Whittle	0.021	0.015	0.015	0.016	0.017	0.018	0.018	0.018	0.018
Second Moment	0.004	0.004	0.004	0.003	0.003	0.004	0.004	0.009	0.026
Ratio	0.027	0.025	0.023	0.021	0.019	0.018	0.018	0.022	0.031
Quadrant	0.045	0.042	0.038	0.034	0.029	0.026	0.025	0.028	0.037
N=625									
Var of Res	0.041	0.045	0.054	0.062	0.071	0.078	0.086	0.093	0.101
Whittle	0.026	0.023	0.024	0.026	0.027	0.028	0.029	0.029	0.029
Second Moment	0.006	0.006	0.005	0.005	0.005	0.005	0.007	0.012	0.030
Ratio	0.040	0.038	0.036	0.033	0.031	0.028	0.027	0.030	0.037
Quadrant	0.063	0.060	0.056	0.051	0.046	0.041	0.040	0.040	0.044
N=312									
Var of Res	0.057	0.061	0.068	0.077	0.086	0.094	0.102	0.109	0.116
Whittle	0.029	0.031	0.034	0.036	0.038	0.039	0.040	0.040	0.038
Second Moment	0.009	0.008	0.008	0.008	0.007	0.008	0.010	0.016	0.034
Ratio	0.058	0.055	0.051	0.047	0.043	0.040	0.039	0.040	0.045
Quadrant	0.092	0.088	0.080	0.070	0.065	0.057	0.050	0.049	0.053
N=156									
Var of Res	0.077	0.080	0.088	0.098	0.109	0.121	0.133	0.144	0.153
Whittle	0.037	0.044	0.048	0.051	0.053	0.055	0.057	0.057	0.056
Second Moment	0.012	0.011	0.011	0.010	0.010	0.010	0.012	0.019	0.039
Ratio	0.076	0.071	0.066	0.061	0.056	0.052	0.051	0.053	0.056
Quadrant	0.118	0.109	0.103	0.097	0.089	0.080	0.072	0.067	0.066
N=78									
Var of Res	0.128	0.126	0.132	0.141	0.153	0.165	0.176	0.184	0.193
Whittle	0.048	0.061	0.068	0.073	0.077	0.079	0.080	0.079	0.080
Second Moment	0.016	0.015	0.015	0.014	0.014	0.015	0.018	0.026	0.047
Ratio	0.106	0.100	0.094	0.088	0.082	0.076	0.072	0.070	0.071
Quadrant	0.194	0.174	0.159	0.151	0.130	0.113	0.100	0.089	0.774
N=39									
Var of Res	0.232	0.229	0.231	0.237	0.246	0.258	0.268	0.279	0.290
Whittle	0.084	0.102	0.115	0.124	0.131	0.135	0.136	0.133	0.133
Second Moment	0.023	0.022	0.021	0.020	0.019	0.020	0.024	0.033	0.054
Ratio	0.161	0.152	0.143	0.134	0.124	0.114	0.106	0.101	0.096
Quadrant	0.289	0.271	0.238	0.225	0.190	0.169	0.147	0.364	1.365

Estimated Standard Deviation **Paths=500**

Technique	H=0.1	H=0.2	H=0.3	H=0.4	H=0.5	H=0.6	H=0.7	H=0.8	H=0.9
N=10,000									
Var of Res	0.006	0.009	0.012	0.015	0.017	0.019	0.021	0.022	0.023
Whittle	0.005	0.005	0.006	0.006	0.006	0.006	0.007	0.007	0.007
Second Moment	0.001	0.001	0.001	0.001	0.001	0.001	0.002	0.004	0.018
Ratio	0.010	0.009	0.008	0.008	0.007	0.007	0.007	0.011	0.020
Quadrant	0.016	0.014	0.014	0.012	0.011	0.010	0.010	0.013	0.024
N=5,000									
Var of Res	0.007	0.012	0.017	0.020	0.024	0.027	0.030	0.032	0.034
Whittle	0.007	0.007	0.008	0.008	0.009	0.009	0.009	0.009	0.009
Second Moment	0.002	0.002	0.002	0.002	0.002	0.002	0.002	0.006	0.021
Ratio	0.013	0.012	0.012	0.011	0.010	0.009	0.009	0.014	0.022
Quadrant	0.021	0.020	0.018	0.017	0.015	0.014	0.014	0.016	0.028
N=2,500									
Var of Res	0.011	0.018	0.024	0.029	0.033	0.037	0.040	0.043	0.046
Whittle	0.010	0.011	0.012	0.012	0.013	0.013	0.014	0.014	0.014
Second Moment	0.003	0.003	0.003	0.002	0.002	0.003	0.003	0.007	0.020
Ratio	0.019	0.018	0.017	0.016	0.015	0.014	0.013	0.016	0.024
Quadrant	0.031	0.029	0.028	0.026	0.023	0.021	0.019	0.021	0.030
N=1,250									
Var of Res	0.015	0.026	0.034	0.042	0.048	0.053	0.057	0.062	0.066
Whittle	0.014	0.014	0.015	0.016	0.017	0.018	0.018	0.018	0.018
Second Moment	0.004	0.004	0.004	0.003	0.003	0.004	0.004	0.009	0.025
Ratio	0.027	0.025	0.023	0.021	0.019	0.018	0.018	0.022	0.029
Quadrant	0.045	0.042	0.038	0.034	0.029	0.026	0.025	0.028	0.036
N=625									
Var of Res	0.022	0.036	0.049	0.059	0.068	0.076	0.083	0.091	0.098
Whittle	0.021	0.022	0.024	0.026	0.027	0.028	0.028	0.029	0.028
Second Moment	0.006	0.006	0.005	0.005	0.005	0.005	0.007	0.012	0.030
Ratio	0.040	0.038	0.036	0.033	0.031	0.028	0.027	0.029	0.034
Quadrant	0.063	0.060	0.056	0.050	0.046	0.041	0.040	0.040	0.044
N=312									
Var of Res	0.027	0.043	0.056	0.068	0.078	0.087	0.095	0.102	0.109
Whittle	0.028	0.031	0.034	0.036	0.038	0.039	0.040	0.040	0.037
Second Moment	0.009	0.008	0.008	0.008	0.007	0.008	0.010	0.016	0.033
Ratio	0.058	0.055	0.051	0.047	0.043	0.040	0.038	0.039	0.041
Quadrant	0.092	0.088	0.080	0.070	0.065	0.057	0.050	0.049	0.052
N=156									
Var of Res	0.038	0.056	0.073	0.087	0.101	0.114	0.126	0.137	0.146
Whittle	0.037	0.044	0.048	0.051	0.053	0.055	0.056	0.055	0.048
Second Moment	0.012	0.011	0.011	0.010	0.010	0.010	0.012	0.019	0.038
Ratio	0.076	0.071	0.066	0.061	0.056	0.052	0.051	0.052	0.051
Quadrant	0.118	0.109	0.103	0.097	0.089	0.080	0.072	0.067	0.065
N=78									
Var of Res	0.055	0.075	0.094	0.111	0.129	0.144	0.156	0.165	0.174
Whittle	0.046	0.061	0.068	0.073	0.077	0.078	0.078	0.074	0.063
Second Moment	0.016	0.015	0.015	0.014	0.014	0.015	0.018	0.026	0.045
Ratio	0.105	0.100	0.094	0.088	0.081	0.076	0.072	0.068	0.063
Quadrant	0.189	0.172	0.158	0.150	0.130	0.113	0.099	0.089	0.766
N=39									
Var of Res	0.120	0.142	0.163	0.184	0.204	0.223	0.239	0.254	0.268
Whittle	0.079	0.101	0.115	0.124	0.130	0.133	0.132	0.125	0.110
Second Moment	0.023	0.022	0.021	0.020	0.019	0.020	0.024	0.033	0.053
Ratio	0.161	0.152	0.143	0.134	0.124	0.114	0.105	0.097	0.086
Quadrant	0.287	0.270	0.237	0.224	0.190	0.169	0.147	0.362	1.315

Estimated Bias Paths=500

Technique	H=0.1	H=0.2	H=0.3	H=0.4	H=0.5	H=0.6	H=0.7	H=0.8	H=0.9
N=10,000									
Var of Res	0.032	0.024	0.018	0.015	0.012	0.010	0.009	0.009	0.008
Whittle	-0.019	-0.005	-0.001	-0.001	-0.001	-0.001	-0.001	-0.001	-0.001
Second Moment	0.000	0.000	0.000	0.000	0.000	0.000	0.000	0.000	0.002
Ratio	0.000	0.000	0.000	0.000	0.000	0.000	0.000	0.000	-0.004
Quadrant	0.001	0.001	0.001	0.000	0.000	0.000	0.000	0.000	-0.001
N=5,000									
Var of Res	0.033	0.024	0.019	0.015	0.013	0.012	0.010	0.010	0.009
Whittle	-0.019	-0.005	-0.002	-0.001	-0.001	-0.001	-0.001	-0.001	-0.001
Second Moment	0.000	0.000	0.000	0.000	0.000	0.000	0.000	0.000	0.003
Ratio	0.000	0.000	0.000	-0.001	-0.001	-0.001	-0.001	-0.002	-0.006
Quadrant	0.000	0.000	0.000	0.000	-0.001	-0.002	-0.001	-0.001	-0.002
N=2,500									
Var of Res	0.033	0.025	0.019	0.015	0.013	0.011	0.010	0.010	0.009
Whittle	-0.017	-0.004	-0.001	0.000	0.000	0.000	0.000	0.000	-0.001
Second Moment	0.000	0.000	0.000	0.000	0.000	0.000	0.000	0.001	0.006
Ratio	0.001	0.000	0.000	0.000	0.000	0.000	-0.001	-0.003	-0.010
Quadrant	-0.001	-0.001	0.000	-0.001	-0.001	0.000	-0.001	-0.002	-0.006
N=1,250									
Var of Res	0.034	0.026	0.021	0.017	0.015	0.013	0.013	0.013	0.014
Whittle	-0.015	-0.003	0.000	0.000	0.000	0.000	0.000	0.000	-0.001
Second Moment	0.000	0.000	0.000	0.000	0.000	0.000	0.000	0.001	0.005
Ratio	0.000	0.000	0.000	0.000	0.000	0.000	-0.001	-0.003	-0.011
Quadrant	-0.001	0.000	0.000	0.000	0.001	0.002	0.001	-0.001	-0.006
N=625									
Var of Res	0.034	0.027	0.023	0.020	0.019	0.019	0.020	0.022	0.026
Whittle	-0.017	-0.005	-0.003	-0.003	-0.004	-0.004	-0.004	-0.004	-0.005
Second Moment	0.000	0.000	0.000	0.000	0.000	0.000	0.000	0.001	0.005
Ratio	0.001	0.000	-0.001	-0.001	-0.002	-0.003	-0.004	-0.005	-0.013
Quadrant	-0.002	-0.002	-0.004	-0.005	-0.006	-0.003	-0.005	-0.005	-0.004
N=312									
Var of Res	0.050	0.043	0.039	0.036	0.035	0.035	0.036	0.038	0.039
Whittle	-0.007	0.001	0.002	0.002	0.001	0.000	-0.001	-0.003	-0.010
Second Moment	0.001	0.000	0.000	0.000	0.000	0.000	0.000	0.002	0.009
Ratio	0.005	0.004	0.003	0.003	0.002	0.000	-0.002	-0.008	-0.019
Quadrant	0.000	-0.002	-0.001	0.000	0.000	-0.001	0.000	-0.004	-0.009
N=156									
Var of Res	0.067	0.056	0.049	0.045	0.043	0.042	0.043	0.044	0.045
Whittle	-0.001	0.000	-0.001	-0.003	-0.006	-0.008	-0.011	-0.016	-0.029
Second Moment	0.000	0.000	0.000	0.000	0.000	0.000	0.001	0.002	0.009
Ratio	0.002	0.000	-0.001	-0.002	-0.004	-0.005	-0.007	-0.013	-0.024
Quadrant	-0.005	0.000	-0.002	-0.005	-0.003	0.000	-0.004	-0.006	-0.012
N=78									
Var of Res	0.115	0.102	0.092	0.086	0.083	0.081	0.082	0.082	0.083
Whittle	0.012	0.006	0.002	-0.002	-0.007	-0.011	-0.018	-0.028	-0.049
Second Moment	0.001	0.001	0.001	0.001	0.001	0.001	0.001	0.003	0.012
Ratio	-0.011	-0.009	-0.008	-0.007	-0.006	-0.006	-0.009	-0.016	-0.031
Quadrant	-0.044	-0.029	-0.018	-0.012	-0.006	-0.007	-0.007	-0.005	-0.106
N=39									
Var of Res	0.199	0.180	0.163	0.149	0.139	0.130	0.121	0.114	0.112
Whittle	0.029	0.014	0.005	-0.003	-0.010	-0.019	-0.030	-0.047	-0.075
Second Moment	0.000	0.000	-0.001	-0.001	-0.001	-0.001	-0.001	0.001	0.010
Ratio	0.004	0.003	0.000	-0.002	-0.006	-0.010	-0.016	-0.026	-0.041
Quadrant	-0.036	-0.029	-0.018	-0.013	-0.005	-0.007	-0.006	-0.034	-0.369

References

[1] Beran, J. (1994). Statistics for Long-Memory Processes, Chapman & Hall, New York.

[2] Brockwell, P.J. and Davis, R.A. (1987). Time Series: Theory and Methods. Springer, New York.

[3] Doukhan, P., Oppenheim, G. and Taqqu, M.S. (2003). Theory and Applications of Long-Range Dependence, Springer, New York.

[4] Embrechts, P. and Maejima, M. (2002). Self-Similar Processes. Princeton University Press, New Jersey.

[5] Hampel, F. (2001). Robust Statistics: A Brief Introduction and Overview. *Robust Statistics and Fuzzy Techniques in Geodesy and GIS Symposium*, ETH Zurich, March 12-16.

[6] Huber, P.J. Ronchetti, E. (2009). *Robust Statistics, Second Edition.* John Wiley & Sons, Hoboken, NJ.

[7] Ledesma, S. and Liu, D. (2000). A Fast Method for Generating Self-Similar Network Traffic. IEEE, 54-61.

[8] Paxson, V. (1997). Fast, Approximate Synthesis of Fractional Gaussian Noise for Generating Self-Similar Network Traffic. Computer Communication Review, 27(5), 5-18.

[9] Peltier, R. and Levy Vehel, J. (1994). A New Method for Estimating the Parameter of fractional Brownian Motion. Institut National de Recherche en Informatique et en Automatique, No. 2396, Programme 4, 1-27.

[10] Peng, C.K, Budlyrev, S.V., Havlin, S., Simons, M., Stanley, H.E. and Goldberger, A.L (1994). Mosaic Organization of DNA Nucleotides. Physical Review E, Vol. 49 (2), 1685-1689.

[11] Taqqu, M.S., Teverovsky, V. and Willinger,W. (1995). Estimators for long-range dependence: an empirical study. Fractals, 3(4):785-789.

[12] Whittle, P. (1961). Gaussian Estimation in Stationary Time Series. Bulletin de l'Institut International de Statistique,Vol. 39, 105-130.

[13] Taqqu, M.S. (1997). Robustness of Whittle-Type Estimators for Time Series with Long-Range Dependence. *Stochastic Models*, Vol. 13, Issue 4, 723-757

[14] Varadhan, S.R.S. (2001). Courant Institute of Mathematical Sciences: Volume 7 Probability Theory, American Mathematical Society, Rhode Island.

[15] Willinger, W., Taqqu, M.S. and Teverovsky, V. (1999). Stock Market Prices and Long-Range Dependence. Finance and Stochastics, Vol. 3, 1-13.